

# Physic and Chemical Transformations for Metal Polymer Nano-composite on Basic Pyrolyzed Polyacrylonitrile (C<sub>3</sub>H<sub>3</sub>N)<sub>n</sub> and Their Impact on Properties

Dmitry Podgorny, Alexey Rodin, Xu Ren

Institute for New Material and Nanotechnology, National University of Science and Technology "MISIS" (Moscow Institute of Steel and Alloys), Moscow, Russian

## Email address:

studoffice@yandex.ru (D. Podgorny), m2002213@yandex.ru (A. Rodin), ip15512422077@gmail.com (Xu Ren)

## To cite this article:

Dmitry Podgorny, Alexey Rodin, Xu Ren. Physic and Chemical Transformations for Metal Polymer Nano-composite on Basic Pyrolyzed Polyacrylonitrile (C<sub>3</sub>H<sub>3</sub>N)<sub>n</sub> and Their Impact on Properties. *Composite Materials*. Vol. 6, No. 1, 2022, pp. 17-31.  
doi: 10.11648/j.cm.20220601.13

**Received:** January 9, 2022; **Accepted:** January 25, 2022; **Published:** February 5, 2022

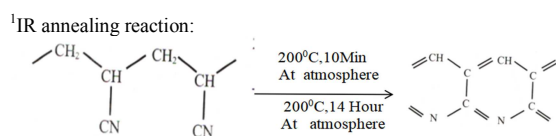
**Abstract:** In this review, we discuss the basic concepts related to various methods (such as Metal Spraying on Polymers, Microencapsulation...) and the properties of electrical Superparamagnetic applied in polymer-metal nanocomposite films. Within the organic-inorganic hybrid nanocomposites research framework, the field related to metal-polymer nanocomposites is attracting much interest. In fact, it is opening pathways for engineering flexible composites that exhibit advantageous electrical, optical, or mechanical properties. The metal-polymer nanocomposites research field is, now, a wide, complex, and important part of the nanotechnology revolution. So, with this review we aim, starting from the discussion of specific cases, to focus our attention on the basic microscopic mechanisms and processes and the general concepts suitable for the interpretation of material properties and structure–property correlations. The review aims, in addition, to provide a comprehensive schematization of the main technological applications currently in development worldwide. So here we show that nanocomposite films of Metal Polymer Based polyacrylonitrile (PAN) films were manufactured using the method of pyrolysis under incoherent IR radiation and were studied using AFM, XPS, and XRD atomic force microscopy (AFM), X-ray photoelectron spectroscopy (XPS), and X-ray diffraction (XRD) methods (Some of those methods are widely used in material research study, here we don't want to introduce them more). The XPS method was used to determine the elemental composition and the chemical and electron states of the elements of the film material. The XRD method showed that the obtained materials contained crystalline inclusions of Me<sub>a</sub>(CO)<sub>b</sub>, Me(CO)<sub>x</sub>(NO)<sub>y</sub> (where Me is a metal) in an organic matrix of PAN. Then by using experimental methods referred in this article, we can achieve a result of polymer pyrolysis, a metal-polymer nanocomposite is formed with nanoparticles less than 100 nm in size, containing a metal or a metal oxide for the research of material properties.

**Keywords:** Physical and Chemical Transformations, Electronic Analyse Method, Metal Polymer Nanocomposite

## 1. Introduction

Physical and chemical transformations occur in process IR annealing<sup>1</sup> on metal polymer nanocomposite and define its physical-chemical property.

For the mechanism of the development of nanocomposite,



it is to research dependencies of structural, superficial, electric, magnetic and optic properties of physical and chemical transformations. So, starting from the introduction of a variety of research methods, we could let beginning researchers interesting in research of Metal Polymer Nano-composite well know about such mechanism. Here are the following research methods:

### 1.1. Methods of Reception of Nanocomposite

Physical-chemical properties of metal polymer nanocomposite depend on categories, concentrations and

nanoparticles' sizes, and are defined with terms of holding synthesis [1-17]. Nanoparticles have properties of intermediate properties of between individual atoms and volumetric materials. Two types of technologies: «top-down» and «bottom-up», are used for creating metal polymer nanocomposites [18]. On the first occurrence way of divisions do they receive volumetric materials of metal polymer nanocomposites [19-22] from assistance of electronic beams or X-ray lithographs. On the second, on the contrary, do they come from atom or molecular made by metal polymer nanocomposites [23-36]. Physic-chemical properties of metal polymer nanocomposites are considered to be created on basic methods of technology «bottom-up».

To technology «bottom-up» relate methods:

1. Microencapsulation of nanoparticles with polymers;
2. Spraying of metal on polymers;
3. Development of metal nanoparticles in polymers with thermal decomposition of precursors;
4. Restorative;
5. Electrochemical;
6. Reception of metal polymer nanocomposite on stages of polymerization (polycondensation);
7. synthesis of metal polymer nanocomposites with bi- and polymetallic nanoparticles;
8. sol-gel;
9. intercalation of polymers in porous and layered nanostructures;
10. Fabrication of metal polymer composites of the inclusions of metal polychalcogenides;
11. Fabrication of metal polymer composites on basic self-organization of molecular structure [24].

### 1.2. Method of Microencapsulation

Method of Microencapsulation consist of creating polymer shells around nanoparticles. Polymer shell carries out functions of stabilizing agent. Thickness of polymer shell depends on method and conditions of microcoacervation [37]. It is for microencapsulation that methods of coacervation and sedimentation with non-solvent or evaporation of solvent use physical adsorption, extrusion and sputtering on fluidized layer, condensation of steams, polymerisation and polycondensation on surfaces of nanoparticles, and also emulsive polymerisation of monomers in presence of nanoparticles [38] or polymerisation of surfacial-active monomers [39], sometimes immobilization of nanoparticles on latex particles [40]. Disadvantages of method consist in scatter of parameters of microcapsules (diameter, thickness of polymer shell and its penetrating ability, heterogeneity of molecular structure) due to the stochastic nature of processes development of polymer microcapsules.

### 1.3. Methods of Metal Spraying on Polymers

To this methods does cryochemical synthesis refer, which includes united low temperature sedimentation of steams of metal and monomer on substrate with following low-temperature solid-phase polymerisation emerging metal

polymer nanocomposite [24-36]. Advantage of such way of synthesis of metal polymer nanocomposite consists in formation of metal nanoparticles, which occurs without involvement of stabilizers, adsorpting on surface of nanoparticles and screening them. In this case is the development of coordination bonds between nanoparticles and polymer matrix also required. Limitation of nanoparticles' size and their immobilization is due to tough lattice polymer matrix, within which their inception and growth occur. Cryochemical synthesis allows to receive metal polymer nanocomposites with concentration of nanoparticles in metal polymer nanocomposites to 50% (approximately). In result does probability of detection and research of important cooperative effects, conditioned interaction between immobilization nanoparticles. With assistance of cryochemical could metal polymer nanocomposites from different nanoparticles, containing Mg, Mn, Ag, Cu, Pd, Pb and PbS [41] synthesize.

By the thermal methods of reception of metal polymer nanocomposites do metallic atoms flow, sprayed on polymer, which locates in potted temperature, created with sublimation or thermal evaporation of volumetric metal by means of thermal heating, ionic spraying, vapor under operation of accelerated electrons, laser pyrolysis. Bombardment of polymer surface with metal atoms accompanied by destruction of their near-surface layers, and sometimes with deep processes of chemical interaction between metal atoms and functional group of polymer. Thermal evaporation is used for sedimentation of nanoparticles not only metal, but also metalloids on polymers. By assistance of such method is Se injected in thin carbon films-with evaporation Se and acrylic acid close to 900°C [42].

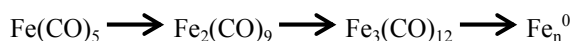
Method of reception of metal polymer nanocomposites on basic plasmonopolymerization and condensation of metal described on work [43].

Polymerisation in smoldering discharge is initiated with ions, excited molecules and photons with sufficient high energy. Difference of plasmonopolymerization from traditional ways of development of polymers-possibility of formation of ultrathin films on omnifarious substrates. Thin films of metal polymer nanocomposites may also be molded in simultaneously polymerization with compound CH<sub>4</sub>, CF<sub>4</sub>, benzene, chlorobenzene, perfluoropropane, hexamethyldisilazane and vacuum evaporation of metals [44]. However it should be noted that polymerisation and condensation of metal steam in low temperature plasma and evaporation are used on described higher methods, which present energetic and economic ineffective operations.

### 1.4. Method for the Formation of Metal Nanoparticles in Polymers by Decomposition of Precursors

This method uses heating of volatile metal-forming precursors (precursors) of carbonyls, carbonylnitrosyls of metals Me<sub>a</sub>(CO)<sub>b</sub>, Me(CO)<sub>x</sub>(NO)<sub>y</sub> (where Me is a metal), formates, acetates,  $\pi$ -allyl complexes, organometallic compounds in organic environments that decompose with the release of metals or oxides in the form of a dispersed phase. In

the case of thermolysis of iron carbonyl, the reaction occurs



Carrying out these reactions in the presence of polymers is a common method of introducing metal nanoparticles into metal-polymer nanocomposites (up to 90 wt%) and preparing ferromagnetic metal-polymer nanocomposites, which is accompanied by chemisorption of the macromolecule on nanoparticles at the moment of their formation [45]. The disadvantage of this method is the toxicity of carbonyls, metal carbonylnitrosyls used as precursors.

### 1.5. Restorative Method

The most common for the production of metal-polymer nanocomposites. Reducing agents of metal ions in the presence of polymers are  $\text{H}_2$ ,  $\text{NaBH}_4$ ,  $\text{NH}_2\text{NH}_2$ , hydrazineborane, phenylhydrazine, hydroquinone, *n*-phenylenediamine, pyrogallol, sodium borohydride,  $\text{LiEt}_3\text{H}$  (where  $\text{Et}=\text{C}_2\text{H}_5$ ), triethylsilane  $\text{Et}_3\text{SiH}$ , various alcohols (more often). Typical metals for the formation of nanoparticles by this method are in the electrochemical series after hydrogen, metal ions with a higher potential are reduced more easily, and it is thermodynamically more advantageous to reduce metal ions with a positive electrochemical electrode potential by hydrogen. It is of interest to use high-molecular-weight reducing agents as reducing agents: polyethyleneimine, polyethylene glycol, poly (N-vinyl-2-pyrrolidone), which could simultaneously perform the functions of both a reducing agent of metal ions and a stabilizer for nanoparticles [46]. However, the introduction of an additional substance into the composition complicates the control of the process. In addition, diffusion limitation of the reduction processes in the polymer matrix significantly lengthens the process in time.

### 1.6. Electrochemical Method

Obtaining metal-polymer nanocomposites is electrochemical polymerization in the presence of metal salts - precursors of nanoparticles, which can also serve as electrochemical activators acting by direct chemical addition to the monomer or by transfer, decomposition, or catalytically [47]. The disadvantage of this method is its sensitivity to impurities, which significantly alter electrochemical processes.

### 1.7. Method of Obtaining Metal-polymer Nanocomposites at the Stage of Polymerization (Polycondensation)

Consists in initiating the polymerization of vinyl monomers and intensive mechanical dispersion of a number of inorganic substances, including metals (Fe, Al, Mg, Cr, W). The degree of conversion of the monomer (styrene, vinyl acetate, acrylonitrile) to polymer depends on the intensity of dispersion. Freshly formed metal surfaces serve as a catalyst or initiator of polymerization: an electron is transferred by surface metal atoms to the monomer with the formation of

initiating particles of the radical ion type. Nanoparticles consisting of Au, Ti, Pt have a catalytic effect on styrene polymerization [48]. The disadvantage of this method is the increased sensitivity of radical polymerization to impurities. Therefore, the combination of polymerization processes and the formation of inorganic nanoparticles seem to be very difficult to reproduce reactions.

### 1.8. Synthesis of Metal-polymer Nanocomposites with bi- and Polymetallic Nanoparticles

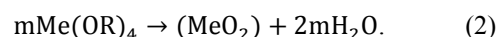
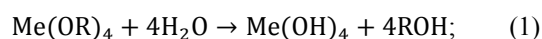
It can be implemented using the methods of obtaining metal-polymer nanocomposites, considered above for the examples of nanoparticles of the monometallic type. For this purpose, cryochemical synthesis is used [49]: a combination of condensation of silver, tin, and methyl methacrylate by vacuum evaporation on a cooled surface of a glass reactor followed by melting and heating obtained metal-polymer nanocomposites with bimetallic nanoparticles with a diameter not exceeding 5 nm. However, this method increases the complexity of the characteristics of the formed products: composition, distribution, morphology, etc. The reduction method is also used to synthesize metal-polymer nanocomposites with bimetallic Pd/Pt- or Pd/Au-nanoparticles [50] upon joint reduction of  $\text{PdCl}_2$  and  $\text{H}_2\text{PtCl}_6$  or  $\text{HAuCl}_4$  in the presence of poly (N-vinyl-2-pyrrolidone): boiling in a water-ethanol mixture, in methanol or irradiation with visible light. The products are stable for 3 months at room temperature, their size is  $\sim 1.5$  and  $3.4$  nm for Pd/Pt and Pd/Au nanoparticles, respectively [51]. As a disadvantage, it should be noted that the methods described above use cryochemical synthesis of the polymer, vaporization of metal vapors, which are energy-intensive and economically ineffective processes.

### 1.9. Sol-gel Method

This is one of the widespread methods for the preparation of metal-polymer nanocomposites. The method is based on polymerization reactions, which include the following main stages:

1. preparation of an initial solution, usually containing metal alkoxides  $\text{Me}(\text{OR})_n$ , where  $\text{Me}=\text{Si}, \text{Ti}, \text{Zr}, \text{Zn}, \text{Al}, \text{Sn}, \text{Ce}, \text{Mo}, \text{W}$ , etc.; R is alkyl or aryl;
2. gel formation;
3. drying;
4. heat treatment.

The hydrolysis reaction is carried out in organic solvents. Subsequent polymerization leads to the formation of a gel:



This method has extremely broad capabilities and allows one to obtain materials containing biologically active macromolecules [52, 53]. The disadvantages include the multistage method, chemically aggressive environment, which makes it difficult to obtain metal nanoparticles without

oxide content.

### 1.10. Nonequilibrium Thermodynamic Methods

In recent years, these methods have been used to create metal – polymer nanocomposites [52, 53]. It is most expedient to use self-organization processes. Polymers representing amorphous substances are characterized by a less ordered structure than crystalline substances, and therefore amorphous substances have higher values of entropy and internal energy. Instability leads not only to the loss of the equilibrium of the system, but also to the manifestation of qualitatively new physical effects, such as the spontaneous generation of order in a disordered system. In order for the system to enter a special regime, in which spatially organized structures are formed, it is necessary that the external influence reaches a certain critical value. This statement is in full agreement with the principles of self-organization and physics of open systems, which were initiated by the work of B. P. Belousov and I. Prigogine [54]. The simplest case, when strongly nonequilibrium states of a solid are formed, are processes occurring when absorption peaks. In the case of a polymer, the radiation frequency should correspond to the range of infrared radiation due to active absorption by organic matter in this region. Under the influence of infrared radiation on PAN, a supramolecular ordered spherulite structure is formed, where the formation of both large (2.5  $\mu\text{m}$  in diameter) and small (200 nm) of spherulites (Figure 1) [55]. The disadvantages of the method include the increased sensitivity of the molecular structure of amorphous substances to external conditions (pressure, temperature, humidity, pH, IR radiation, etc.), which complicate the reproducibility of the method.

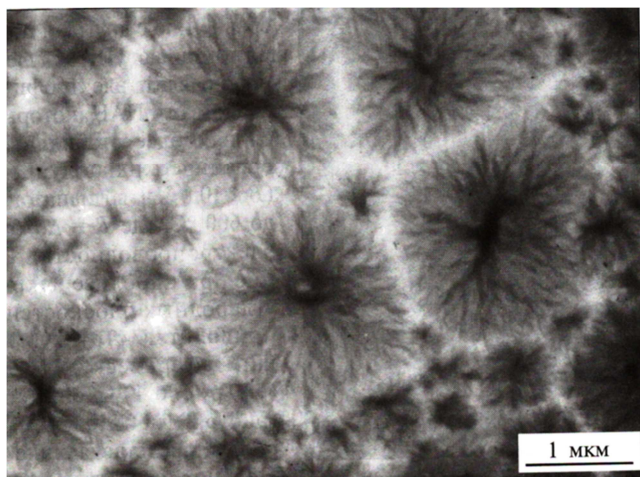


Figure 1. Spherulite supramolecular structure of PPAN.

The development of metal-polymer nanocomposites requires the development of effective methods and manufacturing technologies that determine the reproducibility, quality, and control of the physicochemical properties of the composite. However, the technology for the manufacture of nanocomposites has not been sufficiently studied, and there is a need to investigate the specific

conditions for obtaining nanocomposites and their effect on the physicochemical properties of the composite.

## 2. Experimental Equipment and Methods

### 2.1. Polyacrylonitrile Synthesis Technology and Production of Metal-polymer Composites

The polymer, which is used for the manufacture of metal-polymer nanocomposites, is synthesized according to the technology using a redox catalytic system:  $(\text{NH}_4)_2\text{S}_2\text{O}_8$ - $\text{Na}_2\text{S}_2\text{O}_4$ - $\text{H}_2\text{SO}_4$  [56]. Polymerization is carried out in an aqueous medium at 40°C. Polymerization conditions:  $C_{(\text{NH}_4)_2\text{S}_2\text{O}_8}=1.6 \cdot 10^{-3}$  mol/l,  $C_{\text{Na}_2\text{S}_2\text{O}_4}=6.2 \cdot 10^{-4}$  mol/l,  $C_{\text{H}_2\text{SO}_4}=1.8 \cdot 10^{-2}$  mol/l (Figure 1). The concentration of acrylonitrile monomer is 1.3 mol/l. The loading of acrylonitrile and acid is carried out in two stages: first, distilled water is poured, the catalytic system and 3/4 of the volume of monomer and acid are dissolved. The reaction is carried out in a thermostat at 40°C for 40 minutes. Then charge the rest of the monomer and acid and continue the reaction for 4 hours. The synthesized polymer precipitates out as a white precipitate. The polymer is filtered, washed from sulfuric acid using an aqueous solution of  $\text{K}_2\text{CO}_3$  ( $C=2\%$  (wt.)) Until neutral, and dried under vacuum to constant weight. The molecular weight of PAN synthesized by this technology is  $M_n=1 \cdot 10^5$ . The molecular weight was determined by the viscometric method in a solution of dimethylformamide at a temperature of  $T=30^\circ\text{C}$ . The polymer yield was 50 g.

To prepare a metal-polymer composite, a joint solution of the polymer and metal compounds (oxides, salts) is prepared. Dimethylformamide (DMF) is used as a solvent. The composite is applied to the surface of the substrate, the chemical purity of the surface of which affects the adhesion of the metal-polymer composite. The primary cleaning of the surface is carried out in an ultra- or megasonic bath for 15 minutes using a solution of a surfactant. Solid particles of contaminants with a size of  $\sim 0.3$  microns are effectively removed using a megasound (with a frequency of  $\nu=850$  kHz) at an energy density of 5-10  $\text{W}/\text{cm}^2$ , which is 50 times less than the energy density during low-frequency ultrasonic cleaning ( $\nu=20 \div 80$  kHz). The calculation showed that for megasonic radiation with a power density of 7.5  $\text{W}/\text{cm}^2$  and a frequency of 850 kHz, the time between pulses is 1.1  $\mu\text{s}$ . It is insufficient for the formation of cavitation bubbles. For a time equal to 1 s, the internal energy of the solution changes by 7.5 J. The maximum instantaneous velocity of the molecule under these conditions is 0.9 m/s, and its acceleration is  $8 \cdot 10^5$   $\text{m}/\text{s}^2$ . For half the period, a water molecule moves at a distance of 0.2 microns. Taking into account that the average speed of movement of a molecule is 0.45 m/s, the pressure of megasonic radiation is  $4 \cdot 10^5$  Pa [57]. To remove organic contaminants, a solution of toluene - acetone in a ratio of 3: 1 is used at boiling point for 5 minutes. The solution is applied to the substrate using a centrifuge at the rotation frequency of the substrate with the



applied solution; the film thickness can be varied from 0.02 to 2.0  $\mu\text{m}$ . The substrate with the applied polymer solution containing metal compounds is placed in an oven, where the solvent is removed at 90°C. As a result, a film of a metal-polymer composite is obtained, on the basis of which a nanocomposite is made.

## 2.2. Application of the "Photon" Installation for the Production of Metal-polymer Nanocomposites

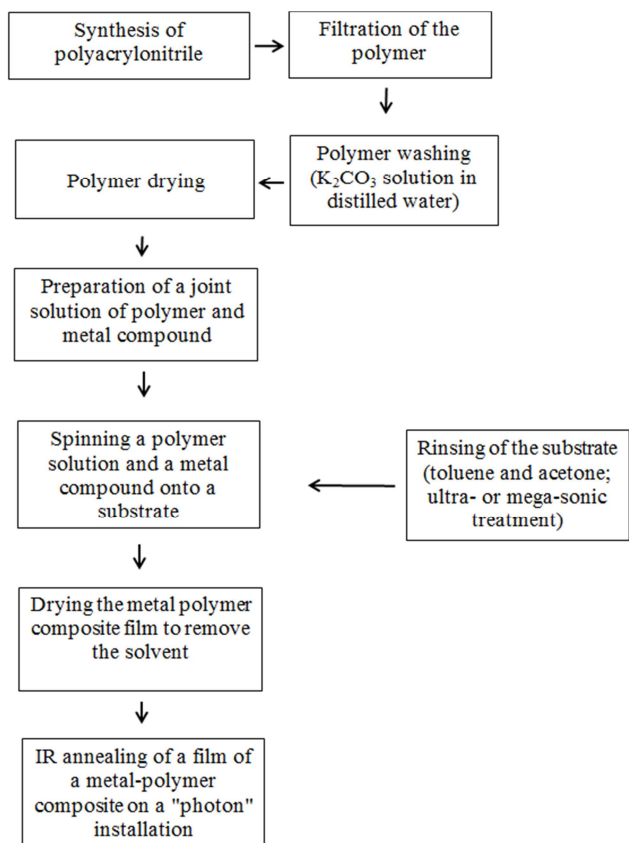


**Figure 1.** Technological scheme for the manufacture of metal-polymer nanocomposites.

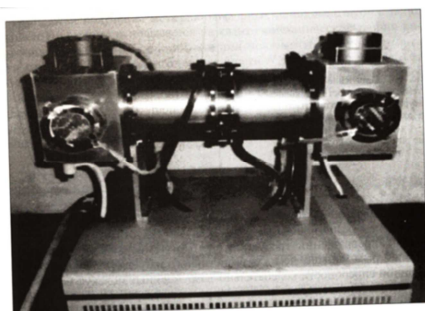


**Figure 2.** General view of the IR annealing unit.

For the manufacture of metal-polymer nanocomposites based on PPAN, the Foton setup (Figure 2), using IR annealing, was used for the first time. The installation is equipped with twelve KG-220 IR lamps with a total power of 12 kW and a maximum radiation intensity in the wavelength range  $\lambda=0.8 \div 1.2 \mu\text{m}$ . A sample placed in a graphite cassette can be heated up to 1300°C with a

temperature rise rate of up to 100 K/min (Figure 3). The IR lamps and electrical contact system are isolated from the reaction zone by a quartz tube-like chamber. This design allows annealing processes to be carried out both in high vacuum and in an atmosphere of active gases (ammonia, hydrogen, oxygen). Thus, it is possible to change the technological conditions of sample annealing depending on the required properties of the metal-polymer nanocomposite. The intensity of the IR radiation was recorded by measuring the temperature using a thermocouple inserted into a graphite cassette. To ensure uniform heating of the sample, the inner surface of the reactor is made of polished aluminum. The "Foton" unit is connected to a computer, with the help of which the software control of the IR annealing technology is carried out with an accuracy of temperature and time measurement of  $\pm 0.1^\circ\text{C}$  and 1 s, respectively. The technical characteristics of the installation give the ability to control with high accuracy the parameters of the metal-polymer nanocomposite formation process and obtain the desired physical and chemical properties of the material. Annealing of the composite is carried out at a pressure of  $P=10^{-1}$  mm Hg. Art. (1 mm Hg=133.322 Pa). At 200°C, the substrate with the metal-polymer composite is kept for 1 hour. Then the temperature is raised to 400°C. As a result of polymer pyrolysis, a metal-polymer nanocomposite is formed with nanoparticles less than 100 nm in size, containing a metal or a metal oxide.

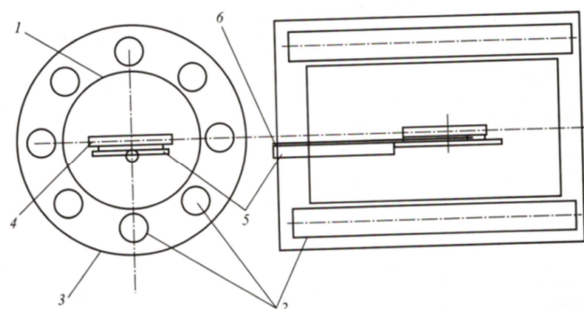


**Figure 3.** Scheme of the IR annealing plant reactor: quartz chamber; 2-halogen lamps; 3- reflective casing; sample; 5-pedestal; 6- tremopar in a quartz tube.

## 3. Results

### 3.1. Thermal Changes in Carbon-carbon, Metal- and Fullerene-polymer Nanocomposites Under the Influence of Infrared Radiation

The discovery of new allotropic forms of carbon - fullerenes and nanotubes - was one of the most remarkable achievements in physical chemistry of the last period. Polymer chains, films, molecular crystallites (fullerides) have been synthesized on the basis of fullerenes. Therefore, fullerenes and nanotubes are often considered as "superatoms" capable of organizing (self-organizing) into condensed systems that have their own structural hierarchy. This approach led to the discovery in 1998 of a new unique class of carbon nanoobjects - peapods, representing a

combination of two types of nanostructures of different dimensions: an ordered ensemble of fullerenes inside carbon nanotubes [58], which are promising as materials for the production of micro- and nanoelectronic products (nanodiodes, transistors, memory elements, logic circuits), high-temperature superconductors [68]. Although amorphous carbons, which may contain heteroatoms, have been studied for many years, their structural properties under thermal transformations have not yet been adequately studied.

Methods of thermogravimetric analysis (TGA), mass spectrometry, X-ray quantitative phase analysis (RQFA), Auger and IR spectroscopy, electron energy loss

spectroscopy (EET), elemental analysis and scanning electron microscopy (SEM) studied the composition of the gas phase during pyrolysis, morphology, chemical composition, chemical structure, surface properties, phase and structural transformations of metal-polymer nanocomposites based on PAN ( $M_n=1 \cdot 10^5$ ), allowing to establish the regularities of their pyrolysis [59-69].

According to mass spectrometry data, substances with molecular weights of 1, 2, 16, 17, 18, 27, 28, 42, 43, 44 were found in the products of PAN pyrolysis. These masses correspond to gaseous pyrolysis products [66, 79]:

Substance	H	H <sub>2</sub>	CH <sub>4</sub>	NH <sub>3</sub>	H <sub>2</sub> O	HCN	CO	C <sub>3</sub> H <sub>6</sub>	C <sub>2</sub> H <sub>4</sub> =NH	CO <sub>2</sub>
Molecular mass	1	2	16	17	18	27	28	42	43	44

At low temperatures, PAN is a chemically stable polymer. In the range of 70-150 and 50-140°C, only H<sub>2</sub>O desorption occurs in vacuum and NH<sub>3</sub> atmosphere, respectively. It is known that nitrile groups actively adsorb H<sub>2</sub>O molecules.

The diffractogram of PAN contains two reflections of the crystalline phase with an interplanar distance  $d_1=0.53$  nm,  $d_2=0.306$  nm and two broad maxima of the amorphous phase with  $d_1=0.343$  nm,  $d_2=0.245$  nm. These parameters correspond to the hexagonal packing of macromolecules. The ratio of crystalline and amorphous phases in the polymer is 1:1. In this case, the value of the coherent scattering regions of polymer crystallites ( $L_{kp}$ ) is 9.5 nm.

When the temperature rises to 140°C under the influence of IR radiation, the quantitative ratio of the crystalline ( $F_{cr}$ ) and amorphous ( $F_{am}$ ) components of PAN does not change (Table 1), and  $L_{cr}$  increases from 9.5 to 11.0 nm. At 175°C,  $F_{cr}$  and  $L_{cr}$  increase to 57% and 13.5 nm, respectively.

**Table 1.** X-ray characteristics of pyrolyzed polyacrylonitrile (PAN) at  $T < 200^\circ\text{C}$ .

sample	T, °C	$\tau$ , min	Phase composition of PAN		
			$F_{cr}$ , %	$F_{am}$ , %	$L_{cr}$ , nm
1	20	-	50	50	9,5
2	140	120	50	50	11,0
3	175	35	57	43	13,5

However, at 200°C, significant changes are observed in the structure of the polymer. The mobility of the hydrogen atom on the tertiary carbon facilitates its migration to the nitrile group with the formation of a methyleneimine group, which forms a hydrogen bond with the nitrile group. The resulting hydrogen bond promotes the formation of a cycle accompanied by the migration of a hydrogen atom along the resulting system of conjugated C=N bonds. In this case, the amorphous zone is energetically more preferable for the cyclization of intril groups than the crystalline region.

With an increase in the duration of irradiation at 200°C, the dehydrogenation reaction of the main chain develops with the formation of conjugated C=C bonds. In this case, the crystalline and amorphous phases of the PAN structure decrease and disappear, and simultaneously other amorphous carbon phases are formed [57] (Table 2):

1. Intermediate phase (Pf), corresponding to a wide halo with a half-width of  $\theta \sim 15^\circ$  and  $d_{\max} \approx 0.3$  nm and characterized by weak scattering of X-rays. (Thus, this phase is a mixture of molecules with different chemical structures and their fragments. In this case, the system has the highest degree of amorphousness);
2. Graphite-like phase (GF) is diagnosed by  $d_{002}G=0.335 \div 0.380$  nm. (Its content increases with an increase in the degree of graphitization Cr. The phase is amorphous due to the irregular displacement of the graphite networks relative to each other in the ab plane and the small size of the regions of coherent scattering of crystallites of the phase GF);
3. Polynaphthenic phase (Hph) is a clathrate structure ( $d \approx 0.47$  nm), consisting of naphthenic rings separated by methylene groups;
4. Phases of unknown structure ( $Y1-d \approx 0.6$  nm,  $Y2-d \approx 0.8$  nm), corresponding to carbon compounds.

The size of the regions of coherent scattering of crystallites of the graphite-like phase and the degree of graphitization of the graphite-like phase in PAPAN increase from 2.1 to 2.7 nm and from 0.58 to 3.38, respectively, the value of  $d_{002}^G$  decreases from 0.371 to 0.343 nm with an increase in temperature from 200 to 600°C.

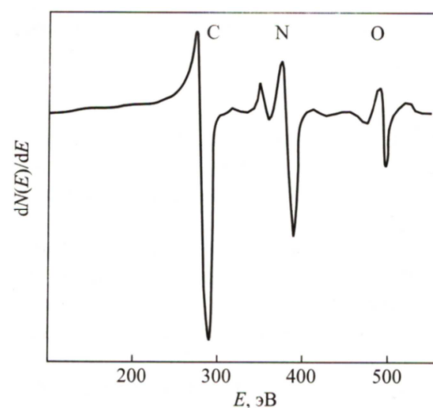


**Figure 4.** Auger spectrum of a PAN film after IR annealing at 600°C in an inert argon atmosphere.

**Table 2.** X-ray characteristics of pyrolyzed polyacrylonitrile at  $T \geq 200^\circ\text{C}$ .

Sample	T, °C	$\tau$ , min	Phase composition of prilled PAN, %					Characteristics of the graphite-like phase ( $G_F$ )		
			$P_F$	$G_F$	$N_F$	$Y_1$	$Y_2$	$d_{002}^G$ , nm	$L_{cr}$ , nm	$C_G$
1	200	30	11	41	41	7	-	0,371	2,1	0,58
2	200	100	14	42	35	9	-	0,371	2,2	0,60
3	600	1/60	-	63	14	11	12	0,343	2,7	3,38
4	700	1/60	-	66	13	11	10	0,345	2,5	2,63

Chemically adsorbed oxygen, forming carbonyl groups, promotes the cyclization of nitrile groups and the formation of a system of polyconjugated bonds. From the survey Auger spectrum, the composition of the PPAN sample  $C_{0.79}N_{0.18}O_{0.03}$  was established, which was pyrolyzed at  $600^\circ\text{C}$  (Figure 4). However, at  $700^\circ\text{C}$ , the  $C_G$  decreases to 2.63, and  $L_{cr}$  - to 2.5 nm, and  $d_{002}^G$  increases to 0.345 nm (see Table 2). According to elemental analysis data [68], the nitrogen content in PPAN sharply decreases from 15 to 7 wt% with an increase in the temperature of IR annealing (IR pyrolysis) from 600 to  $700^\circ\text{C}$ . Due to the increase in defects in PPAN crystallites, the disorder increases, since the coherent scattering region decreases. These data are consistent with the results of the study of PPAN by the SPEE method [61]. The main plasmon energy hop is 22.5, 24.0, and 23.0 eV for PAN samples thermolized at 500, 600, and  $700^\circ\text{C}$ , respectively. With an increase in the annealing temperature from 600 to  $700^\circ\text{C}$ , the energy of the main plasmon decreases from 24.0 to 23.0 eV due to a decrease in the density of valence electrons.

The discovery of a new allotropic form of carbon -

fullerene and tubulenes, which explains the origin of curved carbon planes, spherical and ring-like formations in PPAN, stimulated interest in studying the structural properties of the PAN/ $C_{60}$  composite [52, 55, 59, 60, 62].

To obtain the PAN/ $C_{60}$  nanocomposite, a solution of fullerene  $C_{60}$  in toluene was prepared and then added to a solution of PAN ( $C_{pan}=4$  wt%) in DMF. The mixture was stirred for 20 minutes using an ultrasonic probe. Then the mixture was subjected to IR annealing in an argon atmosphere. In the PAN/ $C_{60}$  composite, the presence of fullerene confirms the presence of characteristic reflections ( $d_{002}=0.835$  nm,  $d_{110}=0.507$  nm,  $d_{220}=0.430$  nm) observed up to  $450^\circ\text{C}$  [56, 70-72].

From the analysis of changes in the X-ray characteristics of the PAN/ $C_{60}$  composite (Tables 3 and 4) during IR annealing, it follows that the initial PAN structure in the composite exists up to  $T=200^\circ\text{C}$ . In this case, the content of the crystalline phase of PAN ( $F_{kr}^{PAN}$ ) gradually increases to 69% and the size of crystallites ( $L_{kp}^{PAN}$ ) to 10.5 nm, and the content of the amorphous phase of PAN ( $F_{am}^{PAN}$ ) decreases to 31%.

**Table 3.** Radiographic characteristics of the PAN/S60 composite under the influence of infrared radiation at  $T \leq 200^\circ\text{C}$ .

Sample	T, °C	$\tau$ , min	Phase composition, %		$L_{cr}$ , nm	$C_{60}$	
			$F_{kr}^{PAN}$	$F_{am}^{PAN}$		$L_{a6}$ , nm	$L_{c6}$ , nm
9	50	10	44	56	9,0	14,5	14,5
10	100	10	47	53	9,5	14,5	15,0
11	125	10	54	46	10,5	16,5	14,5
12	150	10	62	38	10,0	17,5	13,5
13	175	10	69	31	10,5	18,0	13,5
14	200	10	Destruction of PAN			13,5	13,5
15	200	40				160	160

At  $T=200^\circ\text{C}$ , a difference in phase transitions is observed in PPAN and in the composite. Thus,  $P_F$ ,  $G_F$ ,  $N_F$ , and  $Y_1$  are formed in PPAN after IR annealing at  $200^\circ\text{C}$  for a time  $\tau=30$  min. At the same time, the crystalline and amorphous phases of the structure of the initial PAN in the PAN/ $C_{60}$  composite only decrease at  $200^\circ\text{C}$  for 40 min. Thus, no new amorphous

carbon phases are generated. Only after IR annealing for 100 min, the diffractogram reveals reflections of the priolysis phases observed for the  $P_F$ -,  $G_F$ - and  $N_F$ -phases. Probably, cyclization is slowed down (inhibited) in the composite, since fullerene can add hydrogen.

**Table 4.** Radiographic characteristics of the PAN/ $C_{60}$  composite under the influence of infrared radiation at  $T \geq 200^\circ\text{C}$ .

Sample	T, °C	$\tau$ , min	Phase composition, %				$G_F$				$C_{60}$	
			$P_F$	$G_F$	$N_F$	$Y_1$	$d_{002}^G$ , nm	$L_{cr}$ , nm	$C_G$	$L_{a6}$ , nm	$L_{c6}$ , nm	
16	200	100	17	33	44	6	0,362	22	0,81	23,0	31,0	
17	250	10	12	45	37	6	0,362	23	0,83	30,0	31,0	
18	300	10	13	55	27	5	0,360	23	0,92	35,0	28,5	
19	350	10	-	73	20	7	0,345	27	2,70	35,0	28,5	
20	400	10	-	73	20	7	0,345	29	2,90	34,0	35,0	
21	450	10	-	72	14	9	0,344	30	3,33	20,0	20,5	
22	500	10	-	85	15	-	0,343	31	3,90	Sublimation of $C_{60}$ and the formation of an unknown crystalline phase		
23	600	1/60	-	100	-	-	0,341	29	4,85			
24	600	30	-	100	-	-	0,340	29	6,25			

Sample	T, °C	τ, min	Phase composition, %				G <sub>F</sub> d <sub>002</sub> <sup>G</sup> , nm	L <sub>cr</sub> , nm	C <sub>G</sub>	C <sub>60</sub>	
			P <sub>F</sub>	G <sub>F</sub>	N <sub>F</sub>	Y <sub>1</sub>				L <sub>as</sub> , nm	L <sub>c</sub> , nm
25	700	1/60	-	100	-	-	0,344	27	3,00		
26	800	1/60	-	100	-	-	0,344	27	3,00		

As the  $L_{cr}$  and  $C_G$  of the graphite-like phase in PPAN and the composite increase at 600°C, the  $d_{002}^G$  value (see Table 2, sample 3; Table 4, sample 24) decreases. However, at 700°C,  $C_G$  and  $L_{cr}$  decrease, while  $d_{002}^G$  increases for PPAN (see Table 2, sample 4) and composite (see Table 4, sample 25). In this case, the  $C_G$  value for the composite at 600°C (see Table 4, sample 24) is more than twice its value at 700°C (see Table 4, sample 25).

As shown in Tables 3 and 4, the sizes of fullerene crystallites along the a ( $l_a$ ) and c ( $l_c$ ) axes increase under the action of IR annealing.  $l_a$  and  $l_c$  increases from 14.5 to 34.0 and 35.0 nm, respectively, with an increase in temperature from 50 to 400°C. At  $T=450^\circ\text{C}$ , the values of  $l_a$  and  $l_c$  decrease to 20.0 and 20.5 nm, respectively. Reflexes from fullerene disappear at 500°C, and distinct narrow reflections ( $d_1=0.2860$  nm,  $d_2=0.2550$  nm,  $d_3=0.2240$  nm), characteristic of a single crystal of unknown structure (Figure 5), appear in the diffraction spectra composite heated to 500, 600, 700 and 800°C [57]. Apparently, the increasing mobility of fullerenes at 500°C leads to their recrystallization into new crystalline forms, which require further research.

The authors investigated the processes of formation of metal-polymer nanocomposites based on PPAN and transition metals under the influence of incoherent IR annealing. Salts  $\text{FeCl}_3$ ,  $\text{CoCl}_2$  and  $\text{CuCl}_2$ . The introduction of  $\text{FeCl}_3$ ,  $\text{CoCl}_2$  and  $\text{CuCl}_2$  salts into PAN films leads to a decrease in the temperature of phase transformations to 140°C.

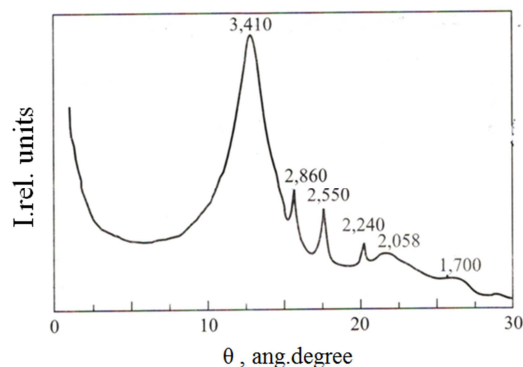


**Figure 5.** X-ray diffraction spectrum of PPAN/C<sub>60</sub> nanocomposite after IR annealing at 600°C.

This may be due to both the catalytic action of metals and the possibility of complexation of the metal with the nitrile groups of the polymer, which significantly changes the nature of the chemical transformations of PAN during heat treatment. When studying the chemical transformations of PAN films under the action of IR annealing in the presence of transition metal chlorides, it was found that these compounds form donor-acceptor complexes of two types with the nitrile groups of the polymer due to the interaction of the d-orbitals of the transition metal either with the lone electron pair of the

nitrogen atom, or with  $\pi$ -electrons of the triple bond  $\text{C}\equiv\text{N}$ . According to the data of IR spectroscopy, there are no absorption bands of stretching vibrations of the free nitrile group in the region of  $2245\text{ cm}^{-1}$ . In this case, two new absorption bands appear in the regions of  $2334$  and  $2191\text{ cm}^{-1}$ , associated with different coordination of the nitrile group. The absence in the IR spectra of an absorption band due to stretching vibrations of the free nitrile group indicates that all nitrile groups are in a complex bound state. The composition of the complexes was determined by the method of molar ratios:  $\text{FeCl}_3(\text{CoCl}_2):(\text{CN})=1:6$  [73].

In this case, the complexation reaction is competitive with respect to the reaction of nitrile groups. Based on the data obtained, an assumption was made that complex-linked nitrile groups should not participate in the cyclization reaction, and in this case a system of conjugated  $\text{C}=\text{N}$  bonds should not form. Indeed, when the films are irradiated with IR light, which provides heating to  $140^\circ\text{C}$ , only a system of conjugated  $\text{C}=\text{C}$  bonds is formed. In this case, nitrile groups do not participate in any chemical transformations. The absence in the IR spectra of absorption bands characterizing the stretching vibrations of the group  $\text{>C}=\text{NH}\dots\text{N}=\text{C}$  in the regions of  $3145$  and  $2215\text{ cm}^{-1}$

confirms the impossibility of the formation of a system of conjugated  $\text{C}=\text{N}$  bonds upon irradiation of PAN films in the presence of transition metal chlorides with low-intensity IR light.... The IR spectra contain absorption bands at  $806$  and  $1380\text{ cm}^{-1}$ , caused by stretching and bending vibrations of the  $\text{—}\overset{\textstyle |}{\text{C}}=\overset{\textstyle |}{\text{C}}\text{—H}$  fragment, as well as a band in the region of  $1600\text{ cm}^{-1}$ , which characterizes the system of conjugated bonds. According to elemental analysis data, the nitrogen content practically does not change.

The ability of nitrile groups in PAN to form complexes with d-metals and their salts offers a simple method for the preparation of metal nanoparticles. Since nanoparticles are unstable due to their nanometer size, they must be stabilized with a polymer matrix that ensures an even distribution of transition metal salts. According to the data of mass spectrometric measurements, the authors found that during thermal transformations in PAN, H and  $\text{H}_2$  are released (Table 5), which reduce  $\text{Cu}^{2+}$  to  $\text{Cu}^0$ .

**Table 5.** The peaks of the partial pressures of  $\text{H}_2$  and H released during the pyrolysis of polyacrylonitrile, and the corresponding temperatures.

T, °C	P, $10^{-4}$ Pa	
	H <sub>2</sub>	H
110	-	1,4
160	5,9	8,0
230	-	3,0
280	4,0	3,5
330	5,2	4,5
390	-	3,7
445	-	2,2
460	4,8	-



T, °C	P, 10 <sup>-4</sup> Pa	
	H2	H
500	5,3	2,1
600	5,7	2,1
670	-	1,6
680	4,7	-
780	-	1,4
800	3,9	-

Under the conditions of the polymer matrix, the aggregation of Cu nanoparticles is difficult due to the complexing activity of the N atom in the PPAN matrix, and the Cu nanoparticles are uniformly distributed in the polymer (Figure 6). According to X-ray diffraction analysis data, Cu nanoparticles ( $d_{111}^{\text{Cu}}=0.2100$  nm,  $d_{200}^{\text{Cu}}=0.1817$  nm) 26 nm in size are formed in the PPAN/Cu metal-polymer nanocomposite at 140°C. It should be noted that repeated annealing of the PPAN/Cu composite at 140°C composite in air does not lead to the formation of copper oxides. Chemically active Cu nanoparticles are stable in air upon heating, since a strong complex of Cu nanoparticles with N atoms in the PPAN matrix is formed and, apparently, the nitriding effect takes place [74].

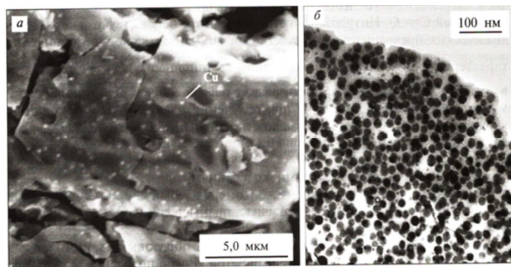


**Figure 6.** Micrographs of PPAN/Cu nanocomposites ( $C_{\text{Cu}}=5\%$  (wt.)) (A) and ( $C_{\text{Cu}}=20\%$  (wt.)) (B), performed using SEM and TEM methods.

### 3.2. Conductive Metal Polymer Nanocomposites

The electrical conductivity of metal-polymer nanocomposites based on a polymer with semiconducting properties and nanoparticles is described by the effect of percolation (flow), i.e., the formation of infinite clusters of conducting particles in the composite structure, through which current flows through the entire sample from one contact to another [75, 76]. The high sensitivity of semiconductor nanoparticles to various external influences (temperature, light, pressure, deformation) in combination with the high elasticity of polymers opens up prospects for the future use of metal-polymer nanocomposites as a new class of solid-state materials for electronics.

The general theory of the percolation effect is based on the concept of the formation of an infinite cluster of conducting nanoparticles in the structure of a metal-polymer nanocomposite. In addition to infinite clusters, shorter clusters are formed along which the transfer of electrons from one external contact to another is impossible. The average size of conducting clusters is characterized by the so-called correlation length  $\xi$ . It was shown in [76] that the percolation cluster has a fractal geometry. The use of fractal geometry made it possible to impart a new meaning to the concept of correlation length, which consists in the fact that the

correlation length determines the boundary spatial scale  $L$ : on scales  $L > \xi$ , the system is homogeneous, i.e.  $N \sim R^d$ , where  $d$  is the dimension of space;  $N$  is the number of particles in the cluster;  $R$  is the characteristic size, and on scales  $L < \xi$  it is a fractal, and in this case the expression  $N \sim R^D$  is valid, where  $D$  is the fractal dimension. Therefore, the dependence of the electrical conductivity on the content of the conducting phase turns out to be nonlinear. Due to the lack of data in the literature, it is of interest to apply the theory of percolation to metal-polymer nanocomposites based on PPAN.

It was found that PPAN is a multiphase mixture [56]. The conductivity of PPAN, which is determined by the content of the G-phase, has been investigated. During annealing using IR lamps, with an increase in the intensity  $I$  of IR radiation, chemical transformations occur, the fraction of Hf increases (see Table 2), and the specific electrical conductivity  $\sigma$  of PPAN increases (Figure 7) [56]. The character of the dependence  $\sigma(I)$  of PPAN coincides with the nonlinear behavior of a similar dependence described by the percolation theory.

If the concentration of conducting particles is zero, then the specific electrical resistances of the composite and the dielectric phase of the polymer  $\rho_d$  are approximately equal. If the concentration of conducting particles is close to 100%, the specific electrical resistance of the composite will be approximately equal to the specific electrical resistance of the material of these particles ( $\rho_m$ ).

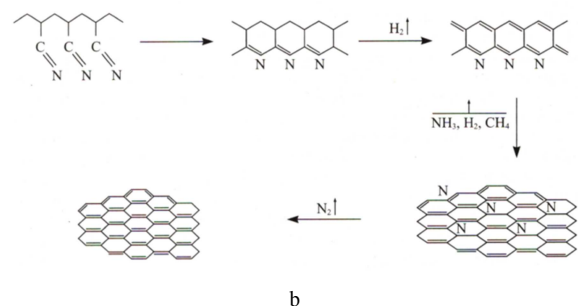
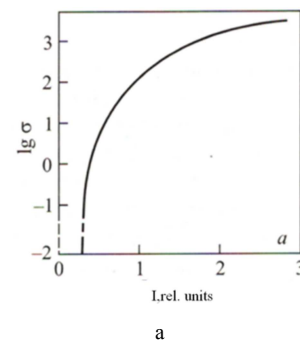


**Figure 7.** Dependence of the specific electrical conductivity in PPAN on the intensity of IR radiation (a) and the chemical transformations corresponding to this dependence (b).

For intermediate concentrations of conducting nanoparticles, the percolation theory [77] gives the dependence

$$\sigma = \sigma_s (x - x_c)^\mu \quad (3)$$

where  $\sigma_s$  is the electrical conductivity of the nanofiller

particle material;  $X$  is the volume fraction of nanofiller particles in the composite;  $X_c$  is the percolation threshold;  $\mu$ -critical index.

From the percolation theory [76] it follows that for spherical particles of both phases with a random chaotic distribution of conducting nanoparticles in the bulk of the composite  $X_c=0.17$  and  $\mu=1.5\div 2.0$ . For the successful experimental implementation of the percolation idea, it is necessary that the adhesion energy of the semiconductor particles with the kinetic units of the E<sub>12</sub> polymer macromolecule exceeds the interaction energy of the E<sub>11</sub> polymer particles with each other:

$$E_{12} > E_{11}. \quad (4)$$

However, if E<sub>12</sub> is large, then the semiconductor nanoparticles will be enveloped by the polymer and significantly hinder the formation of conducting bridges between semiconductor nanoparticles in the cluster.

The conclusions of the percolation theory are confirmed by the electrical properties of a metal-polymer nanocomposite prepared from a joint solution of PAN and AgNO<sub>3</sub> in DMF. Then, from this solution, a polymer film is cast on a copper plate. A reduction reaction takes place between the copper plate and the polymer solution, which contains AgNO<sub>3</sub>, with the production of Ag metal particles:

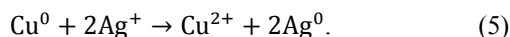


**Table 6.** Dependence of the surface resistivity of metal-polymer nanocomposites based on PAN on the content of AgNO<sub>3</sub>.

Sample	CAgNO <sub>3</sub> , % (the weight.)	$\rho_s$ , Ohm/cm <sup>2</sup>
1	3	$>2 \cdot 10^7$
2	5	$2,2 \cdot 10^1$
3	10	$1,0 \cdot 10^1$
4	15	$4,0 \cdot 10^0$
5	20	$3,6 \cdot 10^0$

The reduction reaction (5) proceeds spontaneously, since the electromotive force or the difference in oxidation potentials for Cu and Ag is a positive number equal to 0.462 V. Films of metal-polymer nanocomposites have a metallic luster and stable electrophysical properties in air for 1 year. At C<sub>AgNO<sub>3</sub></sub> <5% (wt.), The surface electrical resistivity  $\rho_s$  exceeds  $2 \times 10^7$  Ohm/cm<sup>2</sup> (Table 6). With an increase in C<sub>AgNO<sub>3</sub></sub>,  $\rho_s$  decreases by 7 orders of magnitude. Thus, for this case,  $X_c=20\%$  (wt.) [64].

### 3.3. Manufacture of Metal-polymer Nanocomposites Based on Pyrolyzed Polyacrylonitrile Using Infrared Annealing

For the manufacture of metal-polymer nanocomposites, a polymer is required, which has the structure of "entangled" long chains of macromolecules that can easily form a crosslinked spatial structure and chemically interact with metals, forming complexes, which hinders the diffusion and unification of metal atoms. This structure and chemical activity of the polymer helps to control the formation process metal nanoparticles. As a similar polymer, the authors chose PAN, which has the

properties listed above. In addition, during heat treatment in PAN, a polyconjugated system is formed, which ensures the thermal stability of the pyrolyzed form of the polymer up to 2500°C. As a result, with the pyrolyzed form of the polymer up to 2500°C. As a result, during pyrolysis, the mass loss of PAN is significantly lower than that of other polymers. With the help of IR irradiation, it is possible to control the electrophysical properties of PAN, which are the most stable among organic polyconductors ( $R < 10^{-4} \text{K}^{-1}$  in the range from -100 to 600°C, where  $R = \Delta\sigma/(\sigma\Delta T)$ ;  $\sigma$ -electrical conductivity). The formation of curved carbon planes during pyrolysis in PPAN leads to structures that have spherical (spherulites) (see Figure 1), annular (Figure 8), and filamentous (fibrils, representing tubulene-like structures) shapes. Heat treatment of PAN leads to the burnout of disordered areas inside fibrils and spherulites. Thus, fullerene and tubulene-like structures are formed (Figure 9), which can have a size of 2-5 nm [51]. After the discovery of a new allotropic form of carbon, fullerene, PAN pyrolysis is considered as a promising method for creating a new material with semiconducting properties containing fullerene and tubulene-like structures.

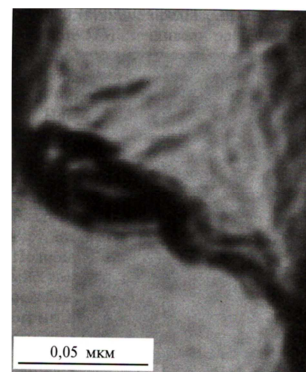


**Figure 8.** Ring-like structure in PPAN.

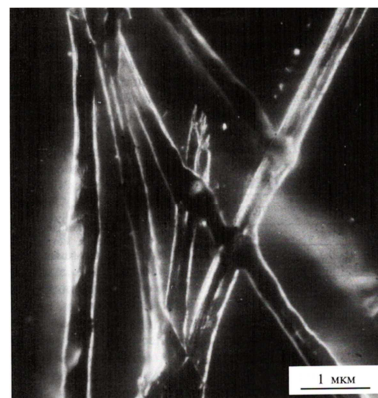


**Figure 9.** Nanometer fibrils in the PPAN structure.

## 4. Discussion

### 4.1. Metal-polymer Nanocomposites with Ferro- and Superparamagnetic Properties

Ferromagnetic metal-polymer nanocomposites play an important role in modern technologies. They are used for the

manufacture of motors, generators, solenoids, devices for microwave electronics, magnetic tomographs, as well as in the field of communications, wireless power transmission. Components made from ferromagnetic metal-polymer nanocomposites are widely used in cars, telephones, microphones, televisions, VCRs, CDs and DVDs, loudspeakers, and computers. Metal-polymer nanocomposites with nanoparticles of ferromagnetic substances Fe, Co, Ni,  $\gamma\text{-Fe}_2\text{O}_3$ ,  $\text{Fe}_3\text{O}_4$  are used as information carriers. One of the advantages of electrospin as a storage medium. One of the advantages of spin-based electronics is that the characteristic length for spin-dependent effects is only 1 nm compared to 10 nm for semiconductor electronics [78]. Nanoparticles of ferromagnetic substances are monodomains isolated in the matrix of a nonmagnetic polymeric material, and the substance passes into a superparamagnetic state. Such substances with a high content of nanoparticles ( $\sim 70\%$  (at.)) Open up new prospects for creating magnetic systems with a high density of recording and storage of information [79]. Calculations show that in a film with nanoparticles  $\sim 5$  nm located on average at a distance of approximately 5 nm from each other, the information density can reach  $\sim 2 \times 10^{12}$  bit/cm<sup>2</sup>. Using the sol-gel method using tetramethylorthosilicate and the  $\text{Co}_3[\text{Fe}(\text{CN})_6]_2$  complex, polymer nanocomposites were obtained, the magnetic properties of which can be changed upon doping with ammonia and illumination [80].

Carbon materials that have ferromagnetic properties have already been predicted theoretically and obtained experimentally [81, 82]. PPAN was prepared by polymerization under the action of  $\gamma$ -radiation in air and by heat treatment from 600 to 900°C in an argon atom. Experimental data indicate a layered structure of this polymer with an interlayer distance of approximately 0.35 nm and the presence of various functional groups grafted onto graphite domains [83]. However, discussions on the magnetic properties of carbon films and their composites continue due to the poor reproducibility of the magnetic properties and the content of impurities in carbon films, and further studies of the magnetic properties of metal-polymer nanocomposites are required.

It is promising to create ferromagnetic metal-polymer nanocomposites based on PPAN and Co, Gd and Fe nanoparticles, since the spin system of the polyconjugated PPAN system provides mechanisms for indirect exchange interaction of non-neighboring metal atoms, forming a kind of "bridges" in combining metal nanoparticles into a single exchange-coupled spin system. In this case, PPAN with a developed polyconjugation system with delocalized  $\pi$ -electrons provides a high density of uncompensated spins. The chlorides Fe and Co introduced into PPAN form donor-acceptor complexes of the  $\pi$ -d and n-d type with the nitrile groups of the polymer. Complex-linked nitrile groups do not participate in the cyclization reaction; therefore, the stage of the formation of conjugated C=N bonds is excluded. The sequences of conjugated double bonds formed as a result of the dehydrogenation reaction of the polymer backbone have a greater length compared to the conjugation regions obtained in the absence of transition metal salts. The use of intense IR

irradiation promotes the acceleration of carbonization processes and the formation of a developed polyconjugation system, the degree of ordering of which is determined by the intensity of IR irradiation. The metal-polymer nanocomposite obtained by the authors based on PPAN and Co nanoparticles (40 wt%) had a specific saturation magnetization of  $13.5 \times 10^{-4}$  T/g. In this case, no hysteresis phenomena were found, which indicates the existence of the formed ferromagnetic compounds in the form of nanoparticles distributed in the organic phase [73].

#### 4.2. Carbon-carbon Nanocomposites for Optoelectronics

Fullerenes can be used as materials for nonlinear optics due to their nonlinear optical properties, which are associated with their extended  $\pi$ -electron conjugation system and strong electron affinity [83]. The dynamics of the change in the photoinduced signal in  $\text{C}_{60}$  fullerene films upon probing with a light flux with a photon energy of  $<1.9$  eV was studied in [84]. On the curves of the time dependence of the differential optical density  $\Delta D(\Delta t)$  at a probing energy in the spectral region of 1.81–2.3 eV, one can distinguish the fast and slow components of the photoinduced absorption. The values of  $\tau_1$  (response time for the fast component) and  $\tau_2$  (for the slow component) for this spectral region are 250 and 720 fs. However, the possibility of manufacturing nonlinear optical devices based on  $\text{C}_{60}$  fullerenes is limited due to their poor solubility and the ability to attach different functional groups [85, 86]. Despite the expanding research on the use of carbon materials in the field of optoelectronics, there are no data in the literature on the optical properties of PPAN.

The authors have studied the optical nonlinear properties of a semiconducting carbon material prepared by thermal treatment of PAN, which dissolves well in many solvents. PPAN is a multiphase mixture of substances that contains nanosized ( $\approx 2.5$  nm) crystallites with graphite-like layers displaced relative to each other (turbostratic phase) [57]. The spectrum of photoinduced absorption in a PPAN film is investigated using femtosecond laser pulses according to the "excitation-probing by a quasi-continuum" scheme. In the experiment, we measured the change in the differential optical density  $\Delta D$  of the film as a result of exposure to a laser pulse with a certain time delay  $\Delta t$ . Photoexcitation of the film was carried out by laser pulses with a duration of 50 fs, an intensity of  $3.1 \times 10^{11}$  W/cm<sup>2</sup>, and an energy of  $h\nu \approx 2.5$  eV. The diameter of the excitation spot was 100  $\mu\text{m}$ . For probing, pulses with a duration of 50 fs in the energy range 1.6–3.0 eV were used. The probing spot was located inside the excitation spot, and its diameter was equal to 50  $\mu\text{m}$ . The repetition rate of the excitation and probing pulses was 2 Hz. The maximum delay in this experiment reached 5 ps [87].

The electronic absorption spectrum for PPAN, obtained by the authors at 600°C (Figure 10, curve 1), is characterized by a small maximum in the energy region of 1.7 eV and intense absorption in the region of 4.0 eV. With an increase in the processing temperature to 700°C (Figure 10, curve 2), strong absorption appears in the region  $E < 2.2$  eV, which may be associated with intense cyclization of the polymer and the formation of a more extended system of conjugated bonds

compared to a film heated to 600°C.

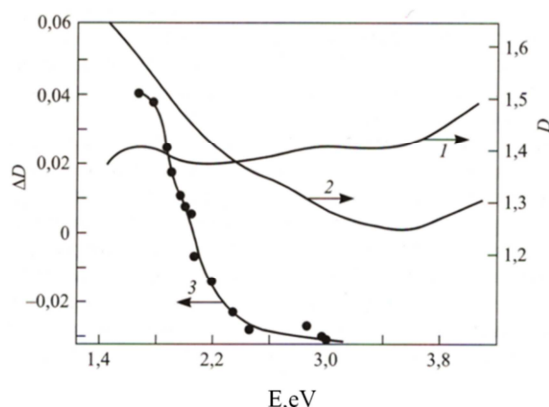


**Figure 10.** Spectra of electronic (1,2) and photoinduced (3) absorption of PPAN films heated by IR radiation to various temperatures  $T$ , °C: 1.3 - up to 600; 2 - to 700.

In the differential optical spectrum (Figure 10, curve 3) at  $\Delta t=0$ , photoinduced absorption is observed in the range of 1.6–2.2 eV, and photoinduced bleaching is observed in the range of 2.1–3.0 eV. With an increase in  $\Delta t$ , the spectrum  $\Delta D(E)$  shifts to the region of high energies  $E$ . At  $\Delta t=3$  ps, the sign of the photoinduced response occurs at 2.3 eV. The experimental data were presented as a sum of two exponentials with damping constants  $\tau_1$  and  $\tau_2$ . It was found that  $\tau_1 \leq 100$  fs,  $\tau_2=400$  fs in the region of photoabsorption of the photoinduced signal in PPAN films when probed with a light flux with  $E < 1.9$  eV is similar to the dynamics of the signal in fullerene films, for which, when probing in the 1.81–2.3 eV region, a fast and slow components of photoinduced absorption. However, the values of  $\tau_1$  and  $\tau_2$  in PPAN films turned out to be several times lower than the corresponding values in fullerene. The short-lived states discovered by the authors at PPAN can correspond to a localized exciton with charge transfer or to an electron plasma formed by a large number of such excitons. Those regions of the film in which excited states appear have their own spectrum and therefore do not participate in the formation of the absorption of the old spectrum. That is why in the spectral region  $E > 2.0$  eV (Figure 10, curve 3), absorption decreases and a photoinduced bleaching signal appears. The photoinduced spectrum in the 1.6–3.0 eV region and a short-lived component with a lifetime of less than 100 fs, discovered for the first time in PPAN, make PPAN films promising for use in optoelectronics [88, 89].

#### 4.3. Sensory Properties of a Carbon Nanocrystalline Semiconductor to the pH of the Medium

Organic semiconductors are intensively studied and used as sensors, using the influence of doping on the change in electrical conductivity, and biosensors with high selectivity and efficiency, since organic semiconductors are compatible and have chemical affinity for enzymes.

According to the measurement data of thermoelectric power, PPAN is characterized by p-type conductivity. The

conduction mechanism in a carbon nanocrystalline semiconductor is explained using electronic states associated with the presence of polarons (radical cations), bipolarons (dication), and solitons, which provide hole conduction. In this case, an electrochemical potential arises in an acidic medium, associated with the equilibrium exchange of p-carriers and protons  $H^+$  of an aqueous solution.

For the first time, the electrochemical activity of PPAN on the pH of the medium was discovered (Figure 11), which can be explained by the formation of a polyconjugated system containing polyaromatic, polyquinoid and isoelefin structures capable of attaching hydrogen, the presence of which leads to the formation of a number of carbon phases contained in PPAN, namely: an intermediate, graphite-like, polynaphthenic, and phases of unknown structure [90]. The possibility of the appearance of curved planes and, consequently, five-membered cycles determines the acceptor properties of a carbon nanocrystalline semiconductor. The slope of the slope in an acidic environment (55–58 mV/pH) is close to the theoretical value (59 mV/pH). In an alkaline environment, the slope drops to 20 mV/pH. Probably, the adsorption of hydroxyl ions  $OH^-$  leads to a change in the electronic states in PPAN and causes a decrease in the sensitivity of properties to the presence of  $H^+$  ions. It should be noted that the approximate direct dependences of the PPAN electrode potential on pH intersect approximately at pH=7, and the electrode potential does not change during the time the electrode is kept in the electrolyte (Figure 12). For graphite and glassy carbon, the dependence on pH is not observed due to their indifferent properties to the electrolyte (see Figure 11).

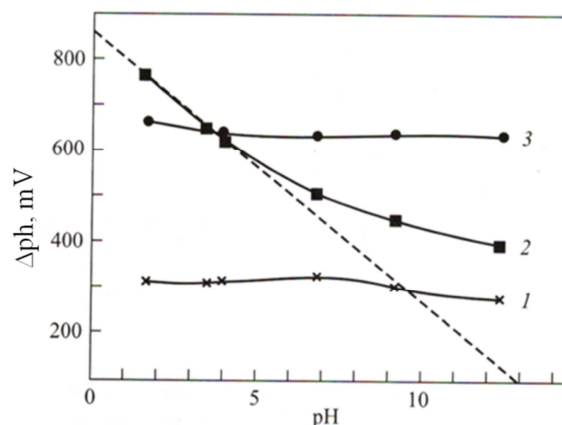


**Figure 11.** Dependences of the electrode potential of graphite (1), PPAN (2), and glassy carbon (3) on the pH of an aqueous solution. The dotted line is the ideal  $\Delta\phi$  (pH) dependence for creating a material with optimal properties (Nerst dependence).

The sensory property makes a carbon nanocrystalline semiconductor promising for the manufacture of pH electrodes used in medicine, biology, and the chemical industry, as well as sensors for the determination of chemically aggressive vapors and gases with acidic or alkaline hydrolysis ( $NH_3$ ,  $H_2S$ ,  $CO_2$ ,  $NO_2$ ,  $HCl$ ,  $Cl_2$ ,  $HF$ ,  $F_2$ ,  $Br_2$ , organosilicon compounds,  $PH_3$ ,  $SO_3$ ,  $SO_2$ ), since PPAN



has high chemical stability in humid, acidic and alkaline media under hyperbaric conditions. In this case, PPAN, having electrical conductivity  $\sigma=10^2$  S/cm, has an advantage over lithium conductive glass with  $\sigma=10^{-12}$  S/cm, used in glass electrodes for measuring pH.

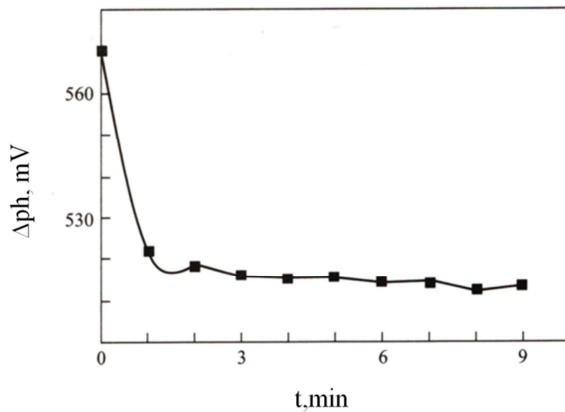


**Figure 12.** Dependence of the PPAN electrode potential on the exposure time in a buffer solution at pH=6.86.

Thus, based on PPAN, the authors obtained metal-polymer nano-composites with the following properties:

1. thickness  $d=0.02 \pm 2.0$   $\mu\text{m}$ ;
2. electrical conductivity  $\sigma=10^{-12} \div 10^4$  S/cm;
3. stability in humid, acidic and alkaline environments under hyperbaric conditions;
4. stability of electrical parameters from -100 to 600°C ( $R < 10^{-4} \text{ K}^{-1}$ );
5. high density  $\rho=1.95 \div 2.0$  g/cm<sup>3</sup>;
6. photoinduced response having a lifetime  $\tau < 100$  fs;
7. specific saturation magnetization of compositions based on PPAN and CoCl<sub>2</sub> (40% (wt.))  $-13.5 \cdot 10^{-4}$  T/g.

## 5. Conclusion

Consequently, the development of nanotechnology based on metal-polymer nanocomposites will contribute to an increase in the economic efficiency of electronics due to the creation of new structures based on these materials with technical characteristics superior to those of structures fabricated using the planar technology.

## List of Abbreviations and Symbols

PAH	Polyacrylonitrile;
IR annealing	Infrared Annealing;
PPAH	acrylonitrile flux cored wire;
DMF	Dimethylformamide;
TGA	thermogravimetric analysis;
RQFA-X	ray quantitative phase analysis;
EET	electron energy loss spectroscopy;
SEM	scanning electron microscopy;
SPEE	Electron energy loss spectroscopy;
GF	Graphite-like phase;
Hph	Polynaphthenic phase.

## References

- [1] Li X., Quan X., Kutal Ch. Synthesis and photocatalytic properties of quantum confined titanium dioxide nanoparticle // Scripta Materialia. 2004. V. 50. P. 499.
- [2] Nyrop S. B., Poulsen M., Veje E. Electroluminescence from Porous Silicon Studied Experimentally // Journal of Porous Materials. 2000. V. 7. P. 267.
- [3] Hulteen, J. C.; Martin, C. R. "A General Template-Based Method for the Preparation of Nanomaterials," J. Mater. Chem., 1997, 7 (7).
- [4] S. W. CHUNG, Y. I. KIM, H. L. PARK and W. J. LEE, J. Mater. Sci.: Mater. Electronics 9 (1998) 383.
- [5] Su, X.; Yau Li, S. F.; O'Shea, S. J. Au Nanoparticle- and SilverEnhancement Reaction-Amplified Microgravimetric Biosensor. Chem. Commun. 2001, 755-756.
- [6] Hao LY, You M, Mo X, Jiang WQ, Zhu YR, Zhou Y, Hu YA, Liu XM, Chen ZY (2003) Materials Research Bulletin 38 (4), 723-729.
- [7] C. Park, J. Yoon, and E. L. Thomas, Enabling nanotechnology with self assembled block copolymer patterns, Polymer, vol. 44, issue. 22, p. 6725, 2003.
- [8] Chapman, R.; Mulvaney, P. Electro-optical shifts in silver nanoparticle films. Chem. Phys. Lett. 2001, 349, 358–362.
- [9] Talin A. A., Dean K. A., Jaskie J. E. //Solid-State Electronics. 2001. V. 45. P. 963.
- [10] Förster, S.; Konrad, M. From self-organizing polymers to nano- and biomaterials. J. Mater. Chem. 2003, 13, 2671.
- [11] Richardson J. N., Aguilar Z., Kaval N. et al. //Electrochimica Acta. 2003. V. 48. P. 4291.
- [12] Grunes, J.; Zhu, A.; Somorjai, G. A. Catalysis and nanoscience. Chem. Commun. 2003, 0, 2257–2260.
- [13] Fang Q., Liu Y., Yin P., Li X. //J. Magnetism and Magnetic Mater. 2001. V. 234. P. 366.
- [14] Sergeev G. B., Shabatina T. I., Low temperature. Surface chemistry and nanostructures, Surf. Sci. 2002, 500, p. 628-655. Shabatina T. I., Sergeev G. B.
- [15] Zheng Y., Ning R. Effects of nanoparticles SiO<sub>2</sub> on the performance of nanocomposites // Materials Letters. 2003. V. 57. P. 2940.
- [16] D. Wei, R. Dave, and R. Pfeffer, J. Nanoparticle Research, 4, 21 (2002). (20) P.
- [17] Pavlov I. N. Creation of crops in the sanitary protection zone of aluminum plants in Central Siberia: Abstract of the thesis. dis. ...cand. s.-x. Sciences. - Leningrad: LTA, 1989. 20 p.
- [18] Cant N. E., Critchley K., Zhang H. -L., Evans S. D. //Thin Solid Films. 2003. V. 31. P. 426.
- [19] Avvakumov EG Mechanochemical methods of activation of chemical processes. -Novosibirsk, 1983.
- [20] Khodakov G. S. Physics of Grinding. - Moscow, 1972.



- [21] Q. Li, E. C. Walter, W. E. van der Veer, B. J. Murray, J. T. Newberg, E. W. Bohannon, J. A. Switzer, J. C. Hemminger, and, R. M. Penner. Molybdenum Disulfide Nanowires and Nanoribbons by Electrochemical/Chemical Synthesis. *The Journal of Physical Chemistry B* 2005, 109 (8).
- [22] Maenosomo S., Okubo T., Yamaguchi Y. Overview of nanoparticle array formation by wetcoating. // *J. of Nanoparticle Research*. 2003. V. 5.
- [23] Peabinder P. A. Selected works. Surface Phenomena in Dispersed Systems (Moscow, 1979) (Colloid Chemistry Series).
- [24] Pomogailo A. D., Rosenberg A. S., Uflyand I. E. Metal nanoparticles in polymers), Moscow, 2000.
- [25] Lin X. M., Wang G. Y., Sorensen C. V., Klaube K. J. // *Journal of Physical Chemistry. B*. 1999. V. 103. P. 5488.
- [26] Dance I. G., Choy A., Scudder I. // *Journal of the American Chemical Society*, vol. 106, issue. 21, p. 6285, 1984.
- [27] Swayambunathan G., Hayes D. H., Schmidt K. et al. // *Ibid*. 1990. V. 112. P. 6285.
- [28] Peyre V., Spalla O., Belloni L., Nabavi M. Stability of a nanometric zirconia colloidal dispersion under compression: effect of surface complexation by acetylacetone // *J. Colloid Interf. Sci*. 1997. - V. 187, N. 1. - P. 184-200.
- [29] Liu S-M, Guo H-Q, Zhang Z-H, Li R, Chen W and Wang Z-G 2000 *Physica E* 8 174.
- [30] Peng X. G., Schlamp M. C., Kdavanich A. V., Alivisatos A. P. // *Journal of the American Chemical Society*. 1997. V. 119. P. 7019.
- [31] Bedja I., Ramat P. V. // *J. Phys. Chem*. 1995. V. 99. P. 9182.
- [32] Qi L., Ma J., Cheng H., Zhao Z. // *J. Phys. Chem. B*. 1997. V. 101. P. 3460.
- [33] Avnir, D.; Braun, S.; Lev, O.; Ottolenghi, M., Enzymes and Other Proteins Entrapped in. Sol-Gel Materials. *Chemistry of Materials* 1994, 6, (10), 1605-1614.
- [34] Pope E. J. A., Braun K., Peterson C. M. // *J. Sol-Gel Science. Technology*. 1997. V. 8. P. 635.
- [35] Pomogailo, A. D., Polymeric Immobilized Metal - complex Catalysts, 1988, 303 p, Moscow Science Publication.
- [36] P. A. Rebinder in an investigation of the mechanical properties of the crystals of calcite and rock salt. *Uzbekistan science*, 1972, vol. 108, issue 1, p. 3.
- [37] Malt V. D. Microcapsulation. - M.: Chemistry, 1980.
- [38] Hasagawa M., Arai K., Saito S. // *Journal of Polymer Science.: Pt A: Polymer. Chemistry*. 1987. V. 25. P. 3231.
- [39] Nagai K., Ohisi Y., Ishiyama K., Kuramoto N. // *Journal of Application of Polymer Science* 1989. V. 38. P. 2183.
- [40] Warshawsky A., Upson D. A. // *Journal of Polymer Science: Pt A: Polymer. Chemistry* 1989. V. 27. P. 2963.
- [41] Ozin G. A., Andrews M. P., Francis C. G. et al. // *Inorganic Chemistry* 1990. V. 29. P. 1068.
- [42] Mendoza D., Lopez S., Granados S., Morales F., Escudero R. // *Synthetic Metals*. 1997. V. 89. P. 71.
- [43] Honorable A. E., Sagaidak D. I., Fedoruk G. G. 1997. V. 39. C. 1199.
- [44] Morosoff N. C., Barr N. E., James W. J., Stephens R. B. // 12 *Internat. symp. on plasma chem. /Eds. by J. V. Hebbelerling, D. W. Ernie, J. T. Roberts. -Minnesota (USA), 1995. -V. 1. P. 147.*
- [45] Smith T. W., Wochick D. // *J. Phys. Chem*. 1980. V. 84. P. 1621.
- [46] Dykman LA, Lyakhov AA, Bogatyrev VA, Shchegolev S. Yu. // *Colloid Journal*. 1998, vol. 39, p. 1199.
- [47] Natanson E. M., Ulberg ZR. Colloid metals and metalpolymers. Kiev: Nauk. dumka, 1971.
- [48] Semchikov Yu. D., Khvatova N. L., Elson V. G., Galliulina R. F. // *Highly medicated. joint A*. 1987. V. 29. P. 503.
- [49] Sergeev B. M., Sergeev G. B., Prusov A. N. // *Mendelev Community*. 1998. N 5. P. 1.
- [50] Toshima N. // *J. Macromol. Science Academic*. 1990. V. 27. P. 1125.
- [51] Harada M., Asakura K., Toshima N. // *J. Physical Chemistry*. 1993. V. 97. P. 5103.
- [52] *The Fractal Approach to Heterogeneous Chemistry Surfaces, Colloids, Polymers/Ed. D. Anvir. N. Y.; Brisbane; Toronto; Singapore, 1997.*
- [53] Nicholis G., Prigogine I. // *Self-organization in nonequilibrium systems. - M., 1979. - P. 545.*
- [54] Bein Th. // *Chemistry of Material*. 1992. V. 4. P. 819.
- [55] Litvinov IA Study of the effect of thermal effects on the supramolecular structure of polyacrylonitrile: Dis.... Candidate of Chemical Sciences/Institute of Chemistry named after A. Topchiev, Academy of Sciences of the USSR, Moscow, 1967.
- [56] Zemtsov L. M., Karpacheva G. P., Kozlov V. V. et al. // *Molecular. Mater*. 1998. V. 10. P. 141.
- [57] Kozlov VV Research and development of technology for colloidal-chemical polishing of the surface of gallium arsenide: Dis.... Candidate of Chemical Sciences/MISIS. - M., 1997.
- [58] Kozlov V. V., Karpacheva G. P., Petrov V. S., Lazovskaya E. V. // *Vysokomolek. Co unit A*. 2001. V. 43. N0 1. P. 23.
- [59] Zemtsov L. M., Karpacheva G. P., Kozlov V. V. et al. // *Abstr. of presentation of Third Internat. Symp. «Polymers for advanced technologies».* -Milan (Italy), 1995. -P. 326.
- [60] Efimov O. N., Krinichnaya E. P., Zemtsov L. M. et al. // *Abstr. of presentation at the Second Internat. Workshop«Fullerenes and atomic clusters».* -St. -Pt. (Russia), 1995. -P. 162.
- [61] Shulga Yu. M., Rubtsov V. I., Efimov O. N. et al. // *Vysokomolek. connections. S-er. A*. 1996. V. 38. N06. P. 989.
- [62] Karpacheva G. P., Zemtsov L. M., Kozlov V. V. et al. // *Abstr. of lectures and oral and poster contributions at 7 Internat. Conf. on Polymer Supported Reactions in organic c-hemistry.* -Wroclaw, 1996. -P. 236.
- [63] Zemtsov L. M., Kozlov V. V., Jawhary T. et al. // *Book of abstr. of 12 Europ. symp. on polymer spectroscopy. - Lyon, 1996. - P. 85.*

- [64] Karpacheva G. P., Zemtsov L. M., Kozlov V. V. et al. //Abstract book of Second Internat. Interdisciplinary Colloquium on the Sci. and Technol. of the Fullerenes. - Oxford, 1996. -P. 58.
- [65] Zemtsov L. M., Karpacheva G. P., Kozlov V. V. et al. //Abstr. of invited lectures and contributed papers. The 3 Internat. workshop in Russia«Fullerenes and atomic clu-sters». -St-Pt (Russia), 1997. -P. 95.
- [66] Bagdasarova K. A., Zemtsov L. M., Karpacheva G. P., Perov N. S., Maksimochkina A. V., Dzidziguri É. L., Sidorova E. N. Structure and magnetic properties of metal-carbon nanocomposites based on IR-pyrolized poly(acrylonitrile) and iron. *Phys. Sol. State* 50 (4) (2008), 750-755.
- [67] Kozlov V. V., Korolev Yu. M., Karpacheva G. P., Efimov O. N. // Abstracts of the report. Of the Fourth Russian Symposium "Liquid Crystalline Polymers". - M., 1999. - P. 60.
- [68] Kozlov V. V., Petrov V. S., Lazovskaya E. V., Pavlov S. A. Conf. "Modern proble-ms of chemistry of high-molecular compounds: high-efficiency and environment-ally friendly processes for the synthesis of natural and synthetic polymers and ma-terials based on them. " - Ulan-Ude, 2002. -P. 86.
- [69] Kozlov V. V., Karpacheva G. P., Petrov V. S. and others // *Izv. universities. Electron materials. technology.* 2004. N04. P. 45-49.
- [70] Karpacheva G. P., Zemtsov L. M., Kozlov V. V. Efimov O. N. //Abstr. of presentati-ons of Second East Asian Symp. on Polymers for Adv. Technol. – Seuol (South Ko-rea), 1999. -P. 61.
- [71] Golyshev V. D., Gonik M. A., Tsvetovsky V. B., Frjazinov I. V., Marchenko M. P. // *Proc. 3rd International Conference on Single Crystal Growth, Strengthen Problems, Heat and Mass Transfer.* Obninsk (Russia), 2000. P. 125—134.
- [72] Korolev YM, Kozlov VV, Polikarpov VM, Antipov E. M. // *Vysokomolek. com-pounds. Ser. A.* 2001. Vol. 43. N011. P. 1933.
- [73] Karpacheva G. P., Zemtsov L. M., Bagdasarova K. A., Muratov D. G., Ermilova M. M. and Orekhova N. V. (2005) Nanostructured carbon materials based on IR-pyrolised polyacrylonitrile, Hydrogen materials scince and chemistry of carbon nanomaterials. ICHMS'2005. IX International Conference, Sevastopol–Crimea – Ukraine, September 05-11, 2005, AHEU, Kiev, 890-891.
- [74] Kozhitov L. V., Krapukhin V. V., Karpacheva G. P., Kozlov V. V. // *Proceedings of universities. Materials of electronic equipment.* 2004. N02. P. 7-10.
- [75] Shklovsky BI, Efros AL *Electronic properties of doped semiconductors.* -M.: Nauka, 1979.
- [76] Vysotsky V. V., Roldugin V. I. // *Colloid journal.* 1998. V. 60. N06. P. 729.
- [77] Fistul V. I. // *Bulletin of Universities, Materials of Electronic Engineering,* 1998, N02, p. 8.
- [78] Jiles D. C. // *Acta Mater.* 2003. V. 51. P. 5907. Han M, Jiles DC, Lee SJ, Snyder JE, Lograsso TA, Schlagel DL. Angular dependence of the unusual first order transition temperature in Gd<sub>5</sub>(Si<sub>x</sub>Ge<sub>1-x</sub>)<sub>4</sub>, Presented at the International Magnetics Conference, Boston, Massachusetts, March 30–April 3, 2003. *IEEE Transactions on Magnetics* 2003; 39 (November) (in press).
- [79] Moore J. G., Lochner E. J., Ramsey C. et al. // *Angewandte Chemie Intern. Ed.* 2003. V. 42. P. 2741-2743.
- [80] Esquinazi, T. The Magnetic Properties of Carbon Material /T. Esquinazi // *Phys. Rev. Lett.* 2003. -V. 22. N. 91. P. 227201-227203.
- [81] Han Y. // *Advanced Material.* 2003. V. 15. N 12. P. 1719-1722.
- [82] Radu Setnescu, Silviu Jipa, Tanta Setnescu et al. // *Carbon.* 1999. V. 37. N 1. P. 1-6.
- [83] Xiao L., Chen Y., Cai R., Huang Z. // *Journal of Material Science Lett.* 1999. V. 18. P. 833-836.
- [84] Cho G. C., Kutt W. // *Physics Review. B.* 1990. V. 42. N 5. P. 2842-2846.
- [85] Chen Y., Huang Z., Cai R., Yu B. // *European Polymer Journal.* 1998. V. 34. P. 137-141.
- [86] Sazanov Yu. N., Mokeev M. V. Novoselova A. V. et al. // *Russian Journal of Applied Chemistry.* 2003. V. 76. N 3. P. 452-456.
- [87] Zhuravleva T. S., Kovalenko S. A., Lozovik Yu. E. et al. // *Book of abstr. Fourth Internat. symp. on Polymer for Advanced Technology –Warsaw (Poland), 1997. -P. PII. 28.*
- [88] Zhuravleva T. S., Zemtsov L. M., Karpacheva G. P. et al., *Chemical Physics.* 1998. T. 17. N06. P. 150.
- [89] Zhuravleva T. S., Kovalenko S. A., Lozovik Yu. E. et al. // *Polymers for Adv. Tech-nol.* 1998. V. 9. N 10-11. P. 613.
- [90] Kozhitov LV, Krapukhin VV, Kozlov VV. et al. // *Coll. scientific and practical. Conf. "Nanotechnology-production". - Fryazino (Russia), 2004.*